Bifiltrations and persistence paths for 2–Morse functions

RYAN BUDNEY
TOMASZ KACZYNSKI

Bifiltrations and persistence paths for 2–Morse functions

RYAN BUDNEY

TOMASZ KACZYNSKI

We study the homotopy type of bifiltrations of compact manifolds induced as the preimage of filtrations of $\mathbb{R}^2$ for generic smooth functions $f: M \to \mathbb{R}^2$. The primary goal of the paper is to allow for a simple description of the multigraded persistent homology associated to such filtrations. Our main result is a description of the evolution of the bifiltration of f in terms of cellular attachments. Analogs of the Morse–Conley equation and Morse inequalities along so-called persistence paths are derived, and a scheme for computing pathwise barcodes is proposed.

1 Introduction

In the past two decades, the Morse theory of smooth functions on manifolds, and singularity theory, its extension to functions with multidimensional values, have driven a lot of attention in the applied mathematics and theoretical computer science communities due to their applications in imaging, visualisation and most recently, topological data analysis (TDA). While those theories have been extensively developed for nearly a century, new and potential applications bring different perspectives.

Morse theory is a tool that allows one to use real-valued functions on a manifold to give a combinatorial description of that manifold, in the language of handle decompositions or CW–complexes. A topological model for M is built following changes in sublevel sets $M_{g \leq y} = g^{-1}((-\infty, y])$ of a Morse function (ie smooth and generic) $g: M \to \mathbb{R}$. The central theorem — see Milnor [22] — about the filtration of M by sublevel sets is that:

(1)   The homotopy type of $M_{g \leq y}$ does not change for $y \in [a, b]$ provided there are no critical values of g in the interval $[a, b]$.

(2) If there is precisely one critical value in (a, b) then the $M_{g \leq b}$ is obtained from $M_{g \leq a}$ by a handle attachment, which up to a homotopy equivalence, is a cell attachment.

In imaging and TDA, the interest shifts to the function itself. The domain of the image is typically a well-understood space such as $\mathbb{R}^n$ or a triangulated sphere S^n. That is a typical setting in works on the shape similarity by size function methods such as in Biasotti, Cerri, Frosini, Giorgi and Landi [4]. When it comes to the study of functions with multidimensional values, there are new challenges and more differences between the classical singularity theory setting and the applied context.

Given the success of Morse theory, the study of generic smooth mappings from manifolds to surfaces $f : M \to \Sigma$ is a natural next step. The most basic elements of the theory involves the description of the stratification of the manifold M by the singularity types, together with the local properties of the mapping around singular points. This was first worked out by Whitney [29] — see also Guillemin and Pollack [16] — when M is a surface, and fully generalized in the subsequent decades; see Saeki [26] and Wan [28]. Perhaps the main difference between the study of functions taking values in $\mathbb{R}$ vs in a surface is that the set of fibres $\{f^{-1}(a) \mid a \in \Sigma\}$ lack a linear order on them, so a poset relation has to be taken into account. In contrast, the real numbers have the relatively canonical poset $\{(\infty, a] \mid a \in \mathbb{R}\}$ of half-infinite intervals.

To be specific, let us state the posets studied in this paper. Consider $f : M \to \mathbb{R}^2$, where M is an m–manifold of dimension $m \geq 2$, and the plane $\mathbb{R}^2$ is endowed with the poset relation
$$(a, b) \preceq (a', b') \iff a \leq a' \text{ and } b \leq b'.$$

Any such function gives rise to a *bifiltration* of M, which is defined as the family $M_f = \{M_{(a,b)}\}_{(a,b) \in \mathbb{R}^2}$ of subsets of M given by
$$M_{(a,b)} = \{p \in M \mid f(p) \preceq (a, b)\}.$$

Equivalently, the sets $M_{(a,b)}$ are the preimages of the quadrants
$$C_{(a,b)} = (-\infty, a] \times (-\infty, b]$$

under f. They are nested with respect to inclusions; that is, $M_{(a,b)} \subseteq M_{(a',b')}$ for every $(a, b) \preceq (a', b')$.

Persistence consists of analyzing homological changes occurring along the bifiltration as the point (a, b) varies. Note that the boundary $\partial C_{(a,b)}$ of the quadrant $C_{(a,b)}$ is

not a submanifold of $\mathbb{R}^2$: it can be viewed as a manifold with a corner. The problem of bifiltration has been addressed in the presented setting by Smale in 1975 [27] and further investigated by Wan [28]. As it is pointed out by Smale, the study is historically motivated by the *Pareto optimal problem* of simultaneously maximizing several functions. Our work is an extension of the work done in [27; 28], with the same topic viewed from a different perspective.

There has been progress in computing persistent homology for multifiltrations which include functions $g\colon M \to \mathbb{R}^k$ as a special case for any $1 < k < \dim M$. We refer the reader to Carlsson and Zomorodian [8] and Cavazza, Cerri, Di Fabio, Ethier, Ferri, Frosini, Kaczynski and Landi [9; 10]. However, most of the dimension-independent work on computing persistent homology, often in a discrete setting, is "geometry blind" in the sense that it does not give much insight to the particular types of singularities one may encounter. Providing that insight is the main motivation for this paper. In particular, in Allili, Kaczynski, Landi and Masoni [1], a Forman-type discrete analogy of multidimensional Morse functions is investigated. In the conclusion of that paper, it is pointed that an appropriate application-driven extension of the Morse theory to multifiltrations for smooth functions is not much investigated yet, and it would help in understanding the discrete analogy. The present work is a step in that direction. A study of discrete Forman type multidimensional Morse functions is currently under way by Landi and Scaramuccia, for instance, in [18]. A study of smooth multifiltrations on manifolds with similar geometric motivation as ours and complementary goals is currently under way by Bubenik and Catanzaro [6] and Assif and Baryshnikov [2].

We begin Section 2 with the definition of a 2–Morse function $f\colon M \to \mathbb{R}^2$, following Gay and Kirby [14] and Wan [28]. This allows us to define the (oriented) signature invariant; see Definition 2.2. We follow this definition with a few simple examples where one can explicitly compute the homotopy types of the filtration $M_{(a,b)}$ for all $(a, b) \in \mathbb{R}^2$. The main result of the paper is a characterisation of the *singular points* of the bifiltration. In short, these are the locations where the homotopy type of the bifiltration changes; see Definition 2.1.

Theorem 1.1 *If* $f\colon M \to \mathbb{R}^2$ *is a 2–Morse function then the bifiltration* M_f *has singular points consisting entirely of corner and tail singular points.*

In short, this theorem gives us a stratification of the plane $\mathbb{R}^2$ such that the homotopy type of $M_{(a,b)}$ is constant in the connected codimension zero strata. We follow that

up by a description of how the homotopy type of $M_{(a,b)}$ changes as (a, b) crosses a codimension one stratum.

Our Lemma 2.8 is the analogue of (1), in that it tells us that generically the homotopy type of the manifolds $M_{(a,b)} = f^{-1}(C_{(a,b)})$ is locally constant. The nature of the proof of Lemma 2.8 is significant to the rest of the paper, describing a rather flexible technique of vector field flows, allowing us to construct conjugate isotopies (ie fibre-preserving isotopies, also known as isotopies that are horizontal diffeomorphisms with respect to the map f) in both M and the plane $\mathbb{R}^2$. This allows us the freedom to frame our remaining arguments in the language of how the homotopy type of $f^{-1}(C_t)$ changes when C_t is an arbitrary "smoothly varying" 2–manifold in the plane. There are however some points in the plane where the homotopy type of $M_{(a,b)}$ does change; this is described in Theorem 2.9. The main feature of Theorem 2.9 is that the homotopy type of $M_{(a,b)}$ changes via handle (or cell) attachments. In the proof we see one of the handle attachments comes directly from a classical Morse theory argument. The second type of handle attachment uses global features of the singular point set of f, and is perhaps best thought of as a Bott-style handle attachment. We give a brief account of Bott's variant of Morse theory. Proposition 2.10 summarizes elements of the proof of Theorem 2.9, describing the dimension of the cell attachments in terms of the oriented signature invariant. One last feature of Section 2 is the observation that at "cubic" points $(a, b) \in \mathbb{R}^2$, while the homotopy type of $M_{(a,b)}$ generally does not change, the fibrewise homotopy type (with respect to the map f) does change. Roughly speaking, these cubic points correspond to pairs of cancelling handles (or cells).

In Section 3, we turn our attention to bifiltered persistent homology. We briefly review descriptive techniques, and relations to one-dimensional persistence. In particular, the foliation method that has been introduced in [4] for size functions, used by Cagliari, Di Fabio and Ferri [7] and [10] for multidimensional persistent homology and later named as fibred barcode in the context of persistence modules by [10] and Lesnick and Wright [20]. As it is visible in examples of Section 2, in the presence of the poset relation, there are multiple ways of building the topology of M by crossing different arcs of the critical value set while respecting the poset relation. That leads us to Definition 3.1 of persistence paths. It is a new concept which is somewhat analogous to the mentioned foliation method of [10]. It also can be viewed as an analogy of a flow induced by the generalized gradient in [28], in that our persistence paths apply to functions f which may have cycles in the sense of [28, Definition 6.4 and 6.5]. We prove an analogy of the Morse–Conley equation — see Rybakowski and Zehnder [25] —

in Theorem 3.2, and derive from it Corollary 3.4 on strong Morse inequalities for persistence paths. This gives us a flexible family of Morse inequalities associated to f, extending the work of Wan [28]. We conclude Section 3 by introducing pathwise barcodes in Definition 3.5 and describing a scheme for computing the barcodes based on a small representable subfamily $\mathrm{Rep}(f)$ of all persistence paths. While Carlsson and Zomorodian [8] outline an argument that there is no complete and discrete invariant of multigraded persistent homology, the primary result of this paper strikes a more optimistic note in the case of multifiltrations induced by smooth functions, implying that our filtrations are tame; see Corollary 2.11.

In Section 4 we discuss some possible future research directions.

2 Fold and cubical singularities

In the classical Morse theory of smooth real-valued functions and, respectively, singularity theory of functions with values in a 2–dimensional manifold Σ, a critical point or singular point is a point $p \in M$ at which $Df(p)$ is not of maximal rank. The corresponding point $c = f(p)$ in the target space is called a critical, respectively, singular value of f. The terminology found in the literature is not consistent: sometimes the terms critical and singular are interchanged.

In computational topology, we deal with nonsmoothness and degeneracy, so a topological definition is more appropriate. It is also helpful in describing handle attachments. In addition, in the presence of the poset structure of bifiltrations, as we shall see soon, there is a substantial difference between singularity in the differential sense and criticality in the topological sense. We shall adopt the following definition.

Definition 2.1 A *homotopy regular value* of f *with respect to the bifiltration* of M is a point $(a, b) \in \mathbb{R}^2$ such that, in some neighbourhood $U_{(a,b)}$ of (a, b), for all $(a', b'), (a'', b'') \in U_{(a,b)}$ with

$$(a', b') \preceq (a'', b''),$$

the inclusion $M_{(a',b')} \hookrightarrow M_{(a'',b'')}$ is a homotopy equivalence. If this condition fails, (a, b) is called a *homotopy critical value*.

A weakening of this definition suited to persistent homology is the notion of *homological regular* and *critical values* defined by replacing homotopy equivalence by isomorphism induced in homology. This coincides with the definition of given in [9, Definition 3.4].

When $f : M \to \mathbb{R}$ is a Morse function, the sets of critical points and values in the differential and topological sense coincide. For $\mathbb{R}^2$–valued functions, even the generic ones, they are substantially different. We shall adopt the terms of *singular* points and values for those given by differential definition and *critical* to those given by Definition 2.1. Given $f : M \to \mathbb{R}^2$. we consider the sets

$$Singp = \{p \in M \mid \text{rank } Df(p) < 2\}, \qquad\qquad Singv = f(Singp),$$

$$Critv = \{(a,b) \in \mathbb{R}^2 \mid (a,b) \text{ is homotopy critical}\}, \quad Critp = f^{-1}(Critv).$$

We shall soon see that the arcs of *Singv* along which both coordinates (a, b) increase are homotopy regular, so they are not subsets of *Critv*. The topologically significant arcs are those whose normal vectors have both coordinates of the same sign. Conversely, *Critv* contains horizontal or vertical half-lines passing through the vertex of $C_{(a,b)}$ and "kissing" points on the singularity *Singv* but not contained in it. In Proposition 2.10 we give a classification of different types of criticality.

As we just noticed, Definition 2.1 also applies to points $(a, b) \in \mathbb{R}^2$ which are not necessarily the values of f, that is, are not in the image $f(M)$. For that reason we will refer to them as points rather than values and whether we speak about points in M or in $\mathbb{R}^2$ should be made clear from the context.

Following [11], the set *Critv* will be referred as to the *extended Pareto grid*. We begin with a definition from Gay and Kirby [15; 14], and earlier Wan [28].

Definition 2.2 A 2–*Morse function* (also called Morse 2–function) is a smooth function

$$f : M \to \Sigma,$$

where M is an m–manifold, $m \geq 2$ and Σ is a 2–manifold satisfying a local condition. For any point $p \in M$ there are neighbourhoods $U_p \subset M$ of p in M, $V_{f(p)} \subset \Sigma$ of $f(p)$ in Σ, U_0' of 0 in $\mathbb{R}^m$, and V_0' of 0 in $\mathbb{R}^2$ together with diffeomorphisms $\phi : U_p \to U_0' \subset \mathbb{R}^m$ and $\psi : V_{f(p)} \to V_0'$ with $\phi(p) = \psi(f(p)) = 0$ making the diagram

$$
\begin{array}{ccc}
U_p & \xrightarrow{\ f|_{U_p}\ } & V_{f(p)} \\
\downarrow{\phi} & & \downarrow{\psi} \\
U_0' & \longrightarrow & V_0'
\end{array}
$$

commute, where the bottom horizontal arrow must be one of the following three:

- $(x_1, x_2, \cdots, x_m) \mapsto (x_1, x_2)$; for this, p is a *regular point*.
- $(x_1, x_2, \cdots, x_m) \mapsto (x_1, \pm x_2^2 + \cdots + \pm x_m^2)$; for this, p is a *fold point*.
- $(x_1, x_2, \cdots, x_m) \mapsto (x_1, x_2^3 + x_1 x_2 + \pm x_3^2 + \cdots + \pm x_m^2)$; for this p is a *cubic point*.

Just like with Morse functions, there are elementary transversality conditions equivalent to Definition 2.2 [28, Section 1]. This allows the conclusion that, for any smooth function $f : M \to \Sigma$ where Σ is a 2–manifold, via a small perturbation of f we may convert f into a 2–Morse function, ie 2–Morse functions form an open and dense subset of the space of smooth functions $M \to \Sigma$.

The curves of the fold singularities come equipped with transverse-oriented indices. This is analogous to the index of a critical point of a Morse function, but made slightly more complex by the codomain of our function being $\mathbb{R}^2$.

The index has the form of a triple (v, i, j) where v is a vector transverse to the singular value set, and i is the dimension of the eigenspace that is folded into the v direction, while j is the dimension of the eigenspace that is folded into the $-v$ direction. Thus $i + j = m - 1$. Due to this convention we need the equivalence relation $(v, i, j) \sim (-v, j, i)$. Further notice that due to the nature of the cubic singularity there are two fold-type singularities that merge, with one fold being of type (v, i, j) and the other fold being of the type $(v, i + 1, j - 1)$. In our diagrams we will typically draw the v vectors, and only plot the pair (i, j). In general i is an integer in the set $\{0, 1, 2, \ldots, m - 1\}$; see Figure 1. Our oriented index makes sense only on the fold points. We give a more precise definition in the next paragraph.

An elementary observation that may help the reader acclimatize to 2–Morse functions is the observation that if $S \subset \Sigma$ is a smoothly embedded copy of $\mathbb{R}$, with $f : M \to \Sigma$ a 2–Morse function, then provided S is transverse to the critical values of f, ie disjoint from the cubic points and without "kissing" tangencies to the fold points, then the restriction of f as a map $f^{-1}(\Sigma) \to \Sigma \simeq \mathbb{R}$ is a Morse function. We use this in Section 3 to define persistence paths. It is also used in the proof of Theorem 2.9.

Definition 2.3 Given a Morse 2–function $f : M \to \mathbb{R}^2$, and a point $p \in M$ in the fold singular points,

$$Hf_p : T_p M \otimes T_p M \to \mathbb{R}^2$$

is a bilinear function taking values in a 1–dimensional subspace of $\mathbb{R}^2$, complementary to the image of Df_p. Choosing $v \in \mathbb{R}^2$ spanning this subspace, we can treat Hf_p
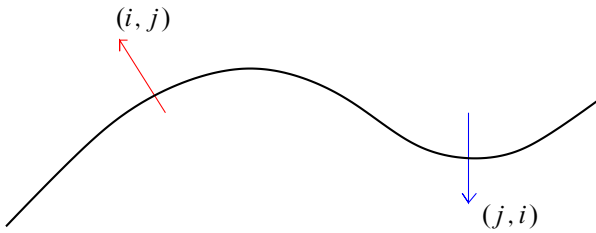
Figure 1: Depiction of the symmetry of the index of fold points.

as real-valued bilinear function, ie by considering $Hf_p \cdot v : T_pM \otimes T_pM \to \mathbb{R}$. As this is a symmetric bilinear function, Sylvester's law of inertia gives us a well-defined signature invariant, (i, j), that can be thought of as the dimensions of the maximal subspaces where the form is positive or negative definite, respectively.

Notice that at a cubic singular point the Hessian is degenerate, ie $i + j = m - 2 < m - 1$, with the nullspace together with the image of Df_p spanning the cusp's plane of curvature.

Before we begin the examples, it is important to be aware that a Morse function $f : M \to \mathbb{R}$ gives rise to a cell decomposition of M [22]. These cell decompositions are computable in terms of flow lines of vector fields conditioned by the derivative of f. The cellular descriptions of M in their most natural state are homotopy-theoretic in nature, ie these techniques give homotopy equivalences between M and CW–complexes, not homeomorphisms. That said, CW–complexes are far from ideal tools to describe manifolds. The adaptation of CW–complexes to smooth manifolds are called *handle decompositions*, developed by Smale in his proof of the h–cobordism theorem. A k–cell for an m–manifold M is a map $D^k \to M$ that satisfies various properties, such as being an embedding on the interior. A k–handle for an m–manifold is a smooth embedding $D^k \times D^{m-k} \to M$, ie handles are not only fully embedded, but they contain the data of both the cell and a tubular neighbourhood of the cell. This allows handle decompositions to not just describe the homotopy type of M, but also its smooth structure. A subtlety of handle attachments is that a k–handle is attached only on part of its boundary, ie $(\partial D^k) \times D^{m-k}$, thus there is a risk that we are entering the class of manifolds with cubical corners. The exposition of Kosinski [17] gives careful consideration to this problem, keeping the constructions purely in the language of manifolds with boundary. A Morse function $f : M \to \mathbb{R}$ gives a handle decomposition of M; moreover this handle decomposition describes the smooth structure on M.

Starting from illustrative examples, we investigate the relation between bifiltration and the classical singularity theory.
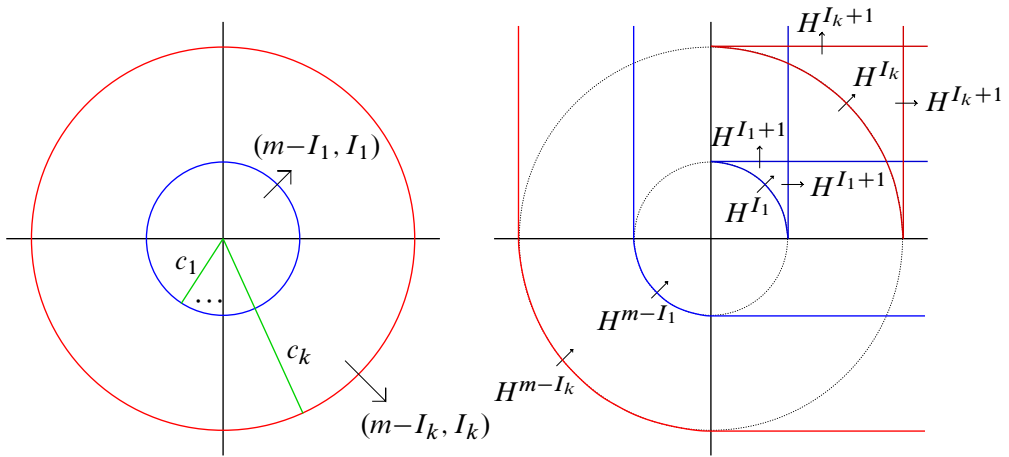
Figure 2: Singular values for f with oriented index in Example 2.4 (left) and extended Pareto grid (right). The dimension of the manifold $S^1 \times M$ is $m + 1$. Only the first and last values, c_1 and c_k, are displayed. The notation H^k indicates k–handle attachments.

Example 2.4 If $g \colon M \to \mathbb{R}$ is a Morse function, then

$$f \colon S^1 \times M \to \mathbb{R}^2$$

given by $f(z, p) = z \cdot g(p)$ is a 2–Morse function on the $(m+1)$–dimensional manifold $S^1 \times M$ with only fold singularity types.

If the singular values of g consist of positive real numbers $0 < c_1 < c_2 < \cdots < c_k$ then the singular values of f consist of the circles of radius $c_1, c_2, \ldots, c_k$ centred at the origin.

If the singular value c_i (of g) has index I_i, then the circle at f of radius c_i is also a fold-type singular value set of index $(\hat{r}, m - I_i, I_i)$, where $\hat{r}$ is the unit outward-pointing radial vector.

The persistence diagram for the preimages $M_{(a,b)}$ is a union of the *descending part* of the singular values of f together with some vertical and horizontal lines at the endpoints.

In Figure 2, the diagram on the left depicts the singular values of the function f. These are the circles of rotation of the singular values of g. Say the red circle corresponds to a singular point of index I_i. An alternative way of saying this is that the homotopy type of the space $g^{-1}((-\infty, t])$ as t transitions through the point c_i changes by an I_i–cell attachment.

In the figure on the right, we describe how the preimages $M_{(a,b)}$ change as the points $(a, b) \in \mathbb{R}^2$ vary. The I_i–handle attachments are labelled by H^{I_i}. Only a portion of
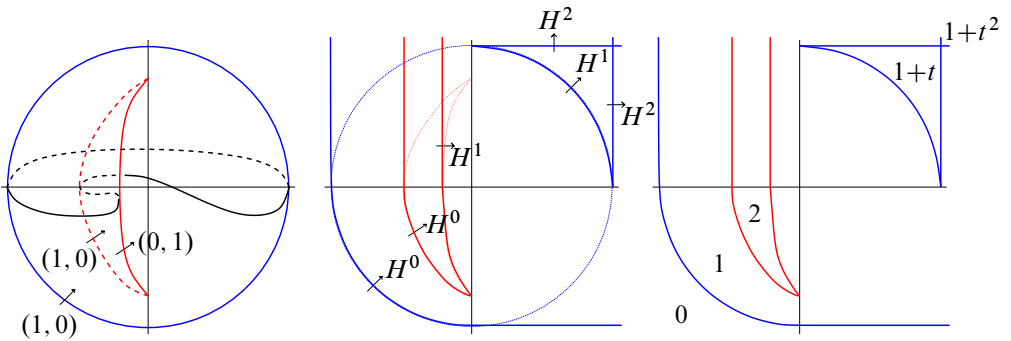
Figure 3: Cupped sphere projection.

the circle from the left diagram remains in the right, since at those (dotted) points the homotopy type of the filtration does not change.

Let us take the blue circle for example, on the left. This is the singular value c_1 of index I_1. On the right, this singular circle gives us two singular arcs. The lower blue arc is properly embedded in $\mathbb{R}^2$, and transitioning through it corresponds to a $m - I_1$ handle attachment. This should be thought of as a dual handle to c_1 (of g). The other singular value is a "fishtail", divided into three properly embedded arcs. The round arc corresponds to a handle attachment of index I_1, while the two straight lines correspond to handle attachments of index $I_1 + 1$. The handles of index $I_1 + 1$ should be thought of as cancelling handles to the index I_1 handle. Thus attachment of all three handles of index I_1, $I_1 + 1$ and $I_1 + 1$ has the same effect on the homotopy type as a single attachment of a handle of index $I_1 + 1$.

Example 2.5 Given a round sphere $S^2 \subset \mathbb{R}^3$, the orthogonal projection map $\pi : \mathbb{R}^3 \to \mathbb{R}^2$ when restricted to S^2 has singular values the unit circle, corresponding to an equatorial circle in S^2 of singular points. Imagine the sphere being made of rubber. We grab a small section of the sphere (away from the equator) and fold it over itself, creating a cupped sphere. This introduces an eye singularity in the projection map, as depicted in Figure 3.

The pure fold singularity, the equator, is in blue. The red singularity is an "eye" type singularity, with precisely two cubic (cusp) points. This is depicted on the left. In the central figure we describe the handle attachments of the bifiltration. In the figure on the right we describe the Poincaré polynomials of the bifiltration, ie the bifiltration is regular at the white points, with transitions only at the red and blue points.
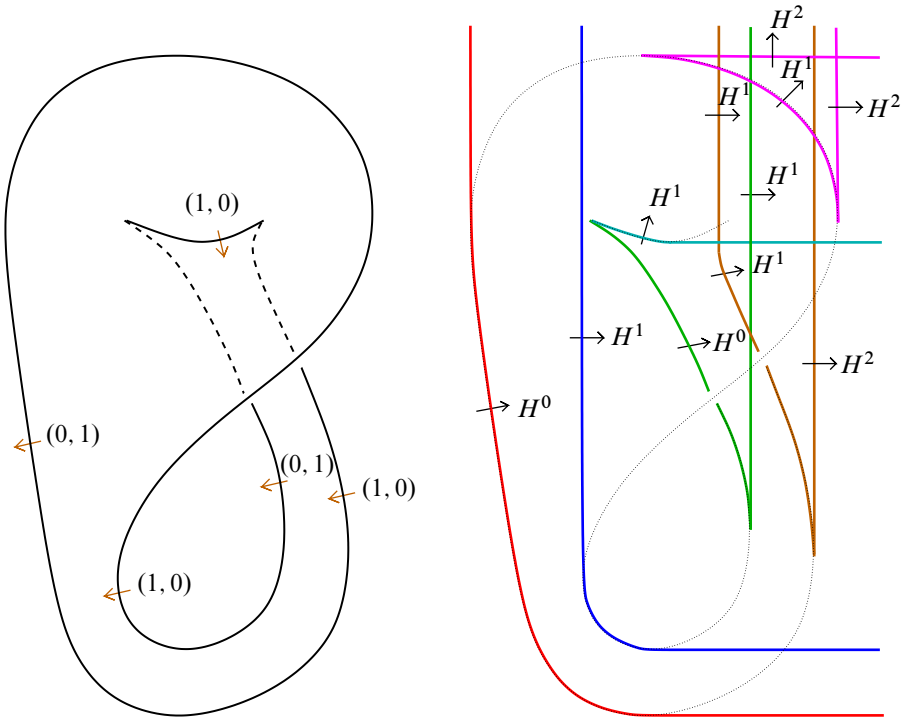
Figure 4: Klein bottle projection.

We give a fairly general example with cubic singularities.

Example 2.6 Cerf theory tells us that a 1–parameter family of real-valued functions on a manifold is not (generically) Morse at all parameter times. There will be finitely many times where the Morse singularities devolve into cubic singularities. Thus take a generic 1–parameter family of functions on M, $F \colon S^1 \to C(M, \mathbb{R})$, and form the function

$$f \colon S^1 \times M \to \mathbb{R}^2$$

given by $f(v, p) = F(v)(p) \cdot v$. The function f is 2–Morse. The bifiltration $M_{(a,b)}$ will be described in Theorem 2.9.

Notice Example 2.6 is a direct generalization of Example 2.4; ie Example 2.4 can be derived by setting F to be the constant function.

Example 2.7 A rather colourful example comes from orthogonal projection $\mathbb{R}^4 \to \mathbb{R}^2$ precomposed with one of the standard embeddings of the Klein bottle $K^2 \to \mathbb{R}^4$.
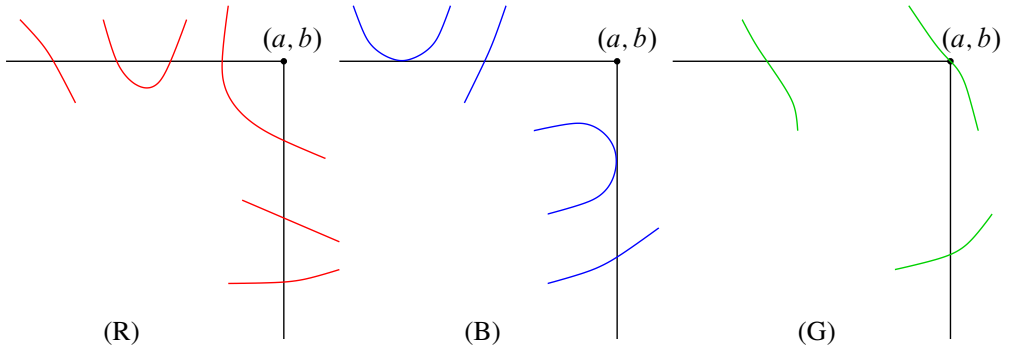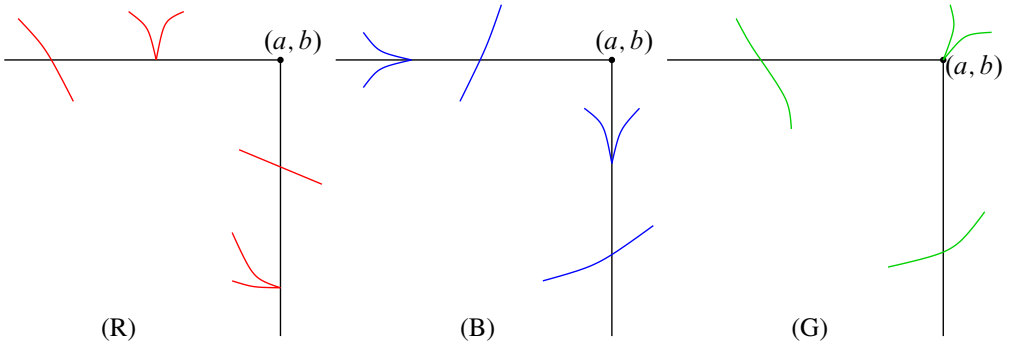
Figure 5: Three intersection types with dimension 1 stratum of the singular values. Type (R) consists of transverse intersections with the 0– and 1–dimensional strata of the singular value set for f. Type (B) consists of both transverse intersections and simple "kissing" nontransverse intersections with the 1–strata of the singular value set. Type (G) consists of transverse intersections together with a corner-type intersection. Thus (R) is generic, ie codimension 0 in the filtration, while types (B) and (G) are of higher codimension.

This example appears in [28]. The singularity theory for mappings of 2–manifolds into the plane, of which this is a good demonstration, was originally discovered by Whitney [29].

We have seen in the previous examples that the singular points of the filtration consist of a subset of the singular points of the mapping f, together with some regular points of the original mapping — these were a collection of vertical and horizontal rays. We divide singular points of the filtration into two classes, *corner singular points* and *tail singular points*:

• We say a point $(a, b) \in \mathbb{R}^2$ is a corner singular point if for all suitably small neighbourhoods U of (a, b) in $\mathbb{R}^2$ there are points $(a', b') \in U$ such that $U \cap C_{(a',b')}$ intersects the singular set of f in both the horizontal and vertical boundary edges of $C_{(a',b')}$. If we write the coordinates of $\mathbb{R}^2$ as (x, y) then this happens when locally writing the singular values of f as the graph of a function $y(x)$, then the function $y(x)$ would be decreasing at $x = a$. A corner singular point is demonstrated in Figure 5(G).

• For (a, b) to be a tail singular point, we require that $C_{(a,b)}$ intersects the singular values of f tangentially, on either the interior of the horizontal or vertical boundary curve. In a neighbourhood of the tangential intersection we require the singular set to be on one side of the cube, ie either contained in the cube or in the closure of its exterior.

Thus it is a "kissing" tangency. The two tail singular point types are demonstrated in Figure 5(B).

Notice that Figure 5(R) describes a regular point (a, b) of the filtration M_f. We should note that while it is true a point can be both corner singular and tail singular at the same time, this is a codimension two condition, thus it is relatively rare. On the other hand, tail and corner singular points are codimension one conditions.

The proof of Theorem 2.9 has several special cases, but there is one elemental argument that is common to all cases. We put this in the next lemma.

Lemma 2.8 *If $f : M \to \mathbb{R}^2$ is a 2–Morse function, provided the point $(a, b) \in \mathbb{R}^2$ is regular for f, and the boundary of $C_{(a,b)}$ intersects the singular values of f transversely without double-points then (a, b) is not only a regular point for the filtration M_f, but the filtration is **locally trivial** near (a, b).*

Proof Precisely, there is a neighbourhood U of $(a, b) \in \mathbb{R}^2$ such that for any $(a', b') \in U$ there is a diffeomorphism $\tilde{\phi} : M \to M$ covering a diffeomorphism $\phi : \mathbb{R}^2 \to \mathbb{R}^2$ such that $\tilde{\phi}(f^{-1}(C_{(a,b)})) = f^{-1}(C_{(a',b')})$ and $\phi(C_{(a,b)}) = C_{(a',b')}$. When we say $\tilde{\phi}$ "covers" ϕ we mean the following diagram commutes:

$$
\begin{array}{ccc}
M & \xrightarrow{\tilde{\phi}} & M \\
\downarrow{f} & & \downarrow{f} \\
\mathbb{R}^2 & \xrightarrow{\phi} & \mathbb{R}^2
\end{array}
$$

The map $\tilde{\phi}$ is sometimes called a fibre-preserving diffeomorphism of f, or a *horizontal* diffeomorphism. A consequence of our proof will be that $\tilde{\phi}$ and ϕ are close to the identity diffeomorphism, where "close" is controlled by the size of the neighbourhood U. That such a neighbourhood exists can be deduced from the transversality stability theorem [16].

The idea of the proof is to find a vector field in the plane whose flow maps $C_{(a,b)}$ to $C_{(a',b')}$ provided (a', b') is near enough to (a, b). We construct the vector field in a manner that allows us to lift it to a vector field on M; thus the flow of this vector field will send $f^{-1}(C_{(a,b)})$ to $f^{-1}(C_{(a',b')})$. Given that the derivative of f is not an epimorphism at singular points of f, we have to take some care defining the vector field. At fold points of f the derivative of f is only onto the tangent space of the singular value set. Thus our neighbourhood U will be constrained by the sole demand

Figure 6: Three intersection types with dimension 0 stratum of the singular values. Type (R) consists of generic outward and inward intersections with the 0–dimensional stratum of the singular value set for f. Type (B) consists of nongeneric intersections with the 0–dimensional stratum. Type (G) consists of a generic corner-type intersection with the 0–dimensional stratum. In the filtration parameters, (G) is of codimension two. Type (B) is of codimension one if it exists, but for a generic 2–Morse function these singularity types are avoidable; one can convert them into type (R) by applying a small isotopy to f.

that the singular value set needs to be transverse to $\partial C_{(a',b')}$ for all $(a',b') \in U$. An example illustration of a valid U is depicted in the green region illustrated is the set of points $UC = \{p \in \partial C_{(a',b')} \mid (a',b') \in U\}$.

For the sake of argument, let's assume $b' = b$, ie we break the proof into two steps, step 1 with $b' = b$ and step 2 with $a' = a$. We further assume $a' > a$ as the $a' < a$ case is analogous. Let $Singv(f)$ denote the singular values of f, ie $Singv(f) \subset \mathbb{R}^2$. Consider the curves of $Singv(f) \cap UC$. On the path-components of $Singv(f) \cap UC$ that live in the vertical portion of UC, we define the vector field to be the unique vector field that is tangent to $Singv(f)$, and whose x–component is, in particular, positive. On the path components of $Singv(f) \cap UC$ that are in the horizontal portion of UC we define the vector field to be zero. In the horizontal portion of UC we extend the vector field to be zero. In the vertical portion of UC we interpolate between the definition on $Singv(f) \cap UC$ and the vector field $(1, 0)$, using a tubular neighbourhood of $Singv(f)$ in UC. Doing this we can ensure the vector field in the vertical portion of UC always has unit x–component. We extend the vector field to all of $\mathbb{R}^2$, choosing any extension that keeps the length of the vector field bounded, ie so that its flow is complete. This gives us a flow on $\mathbb{R}^2$ that sends $C_{(a,b)}$ to $C_{(a',b)}$. Our vector field
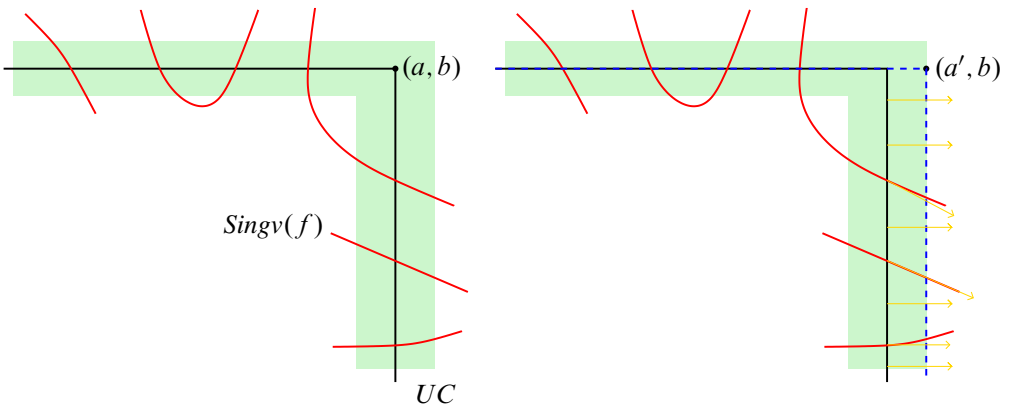
Figure 7: Neighbourhood of $\partial C_{(a,b)}$ and the tangency types for *Singv*.

lifts to M since the derivative of f is onto the tangent spaces of $Singv(f)$, and for regular points, the derivative has rank two. By the existence and uniqueness theorem for solutions to ODEs, the flow of an f–lifted vector field is conjugated (by f) to the flow of the original vector field on $\mathbb{R}^2$. Thus the flow on M is fibre-preserving and sends $f^{-1}(C_{(a,b)})$ to $f^{-1}(C_{(a',b)})$. □

Lemma 2.8 has several natural generalizations. For example, let C and C' be compact 2–dimensional submanifolds of $\mathbb{R}^2$. Then provided there is an isotopy between C and C' such that ∂C is transverse to the singular value set of f through the entire isotopy (technically one needs to include intersections pairs of $Singv(f)$ curves as 0–strata in $Singv(f)$ for this statement to be true), then $f^{-1}(C)$ and $f^{-1}(C')$ are fibrewise diffeomorphic. The condition that the isotopy is transverse to the singular value set through all parameter times guarantees that the boundary of C does not pass over a cubic point, or ever become tangent to the singular value set. These are the events that can trigger changes in the fibrewise homotopy type of the preimage.

Similarly, provided (a, b) is a regular value of f we can *round the corner*, turning $C_{(a,b)}$ into a smooth manifold $C'_{(a,b)}$ such that $f^{-1}(C_{(a,b)})$ and $f^{-1}(C'_{(a,b)})$ are homotopy equivalent.

We choose to let C be a compact submanifold of $\mathbb{R}^2$ for the following arguments; ie rather than working with quadrants $C_{(a,b)}$ we choose to work with compact smooth manifolds, as it exposes the essential features of the argument.

The next theorem states that if the boundary of C (or quadrant $C_{(a,b)}$) passes over a cubic point in the isotopy, the fibrewise homotopy type changes but the homotopy type
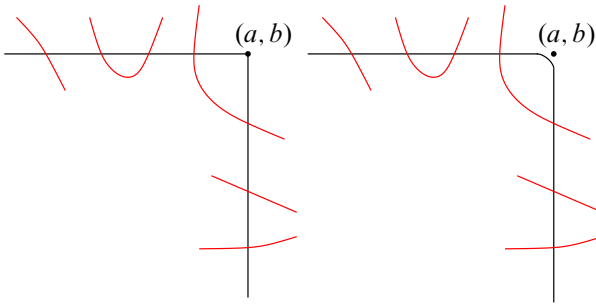
Figure 8: Rounding $C_{(a,b)}$ to produce $C'_{(a,b)}$.

does not. Moreover, if the boundary of C passes across the singular value set — at a tangency or corner, ie Figure 5(B) and (G) — then the homotopy type changes via a cell attachment. We also give enough details that allow the computation of the attaching maps.

Theorem 2.9 *If $f: M \to \mathbb{R}^2$ is a 2–Morse function then the bifiltration M_f has singular points consisting entirely of corner and tail singular points. Further, provided the two height functions $\pi_i: \mathbb{R}^2 \to \mathbb{R}$ given by $\pi_1(x, y) = x$ and $\pi_2(x, y) = y$ restrict to Morse function on the fold singular values of f, with distinct critical heights, then the transitions to the homotopy type of $M_{(a,b)}$ when (a, b) is either a corner or tail singular point are given by individual cell attachments.*

Proof Rather than using the restrictive language of quadrants, let C be a compact submanifold of $\mathbb{R}^2$ and we investigate the change in homotopy type of $f^{-1}(C)$ through an isotopy of C. We have two cases to consider.

Case 1 is a regular tangency — analogous to a type-2 Reidemeister move of the planar diagram, in that it creates two points of intersection between the boundary of C and the singular value set. Roughly speaking, there are two types of regular tangency moves. This move can be described via a "bigon modification" where one appends a bigon to the manifold C, attaching along one of the edges. The second edge of the bigon belongs to $Singv(f)$. In the "nonengulfing" move, $Singv(f)$ points out of C after the bigon is appended, while in the engulfing version, $Singv(f)$ points into C as one departs the bigon.

In the nonengulfing version of case 1, the move corresponds to a cell attachment of index i provided the index of $Singv(f)$ is of the form (v, i, j) where v is in the direction of ∂C as it sweeps over $Singv(f)$.
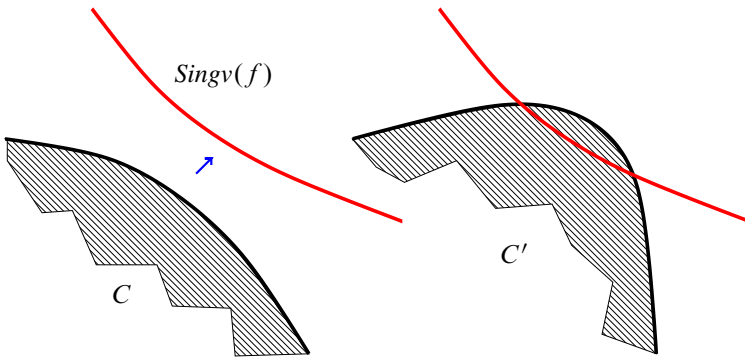
Figure 9: Case 1, nonengulfing.

Let C' denote the submanifold of $\mathbb{R}^2$ after the isotopy of C has been applied, ie as in the right hand side of Figure 8. Using an argument analogous to Lemma 2.8 we see that $f^{-1}(C')$ has the same homotopy type as $f^{-1}(C) \cup f^{-1}(B)$, where B is the blue arc in Figure 10.

The restriction of f to $f^{-1}(B)$, and after identifying B with an interval in $\mathbb{R}$, is a 1–Morse function; thus $f^{-1}(B)$ has the homotopy type of $f^{-1}(B \cap C)$ attach an i–cell, by the Morse lemma. More specifically, this is proven in [22, Theorem 3.2].

For the engulfing version of case 1, the cell attachment is of index $i + 1$ provided the index of $Singv(f)$ is (v, i, j), and the attaching map is analogous to the previous case, but it should be thought of as an unbased version of a Whitehead product of the attaching map in the previous case, with the red interval disjoint from C in the diagram in Figure 11. Specifically, the characteristic map will be a product $D^i \times I$, where the D^i maps transversely to the red interval, and I can be identified with the red interval.
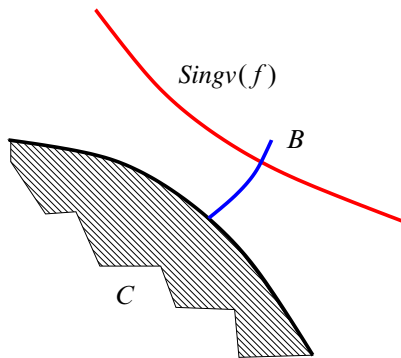
Figure 10: Case 1, nonengulfing.
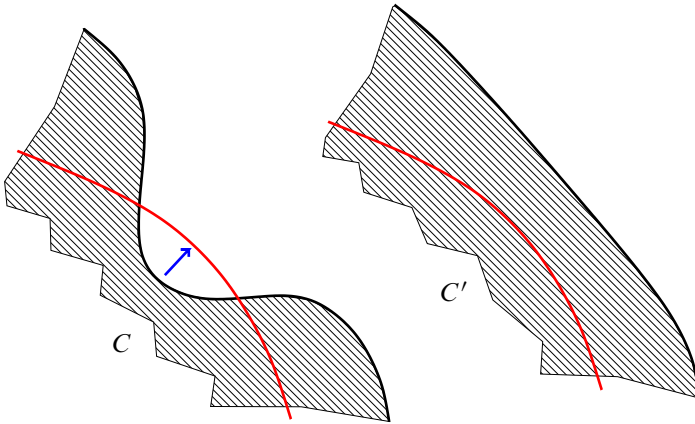
Figure 11: Case 1, engulfing.

Figure 11 indicates the rationale. Specifically, $f^{-1}(C')$ is $f^{-1}(C)$ union a relative Bott-type handle. This handle should be thought of as $I \times D^i \times D^{m-i-1}$, where (v, i, j) is the index of $Singv(f)$. This is because $\pi_v \circ f$ is a Bott-style Morse function on $f^{-1}(B)$; see Figure 12. The function $\pi_v : \mathbb{R}^2 \to \mathbb{R} \cdot v$ is orthogonal projection onto the line spanned by v. The "box" B is diffeomorphic to a product $B \simeq I \times I$ where the first interval factor corresponds to the red arc of $Singv(f)$ disjoint from C in Figure 12, while the second interval I is in the transverse direction (ie can be taken to be parallel to v). Thus $f^{-1}(B)$ is an interval cross an i–handle, being attached to $f^{-1}(C)$ along $(I \times \partial D^i) \cup ((\partial I) \times D^i)$, ie $\partial(I \times D^i)$. This could be thought of as an unbased version of a Whitehead product.

For details on Bott-style Morse functions, and how they give disc-bundle adjunctions for manifolds, see the paper of Bott [5, below (3.6)]. For a gentler introduction, see [3].

Case 2 is the case where the boundary of C passes over a cubic point. We will see that the homotopy type of $f^{-1}(C)$ does not change in this instance. Like case 1 there is are "engulfing" and "nonengulfing" subcases. We restrict to the nonengulfing case, as the engulfing case is similar. The main idea of the proof is that this transition corresponds to a 1–parameter family of cancelling i and $(i+1)$–handle attachments; thus we are attaching a ball along a hemisphere, which results in no change in the homotopy type.

A small variant of Lemma 2.8 occurs when the boundary of C transitions over a double-point in the singular set as in Figure 14. While the fibre homotopy type of $f^{-1}(C)$ changes during this kind of transition, the homotopy type of $f^{-1}(C)$ does not. The proof is exactly as in Lemma 2.8, in that we define the vector fields first on
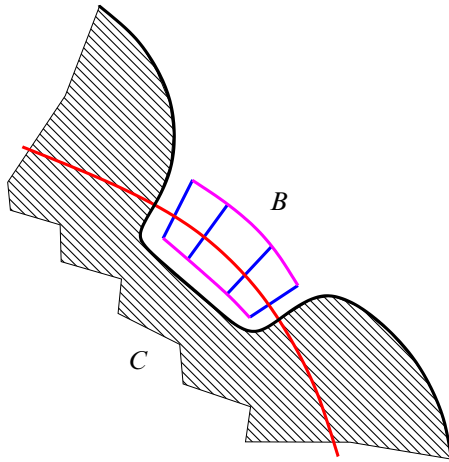
Figure 12: Case 1, engulfing.

the red curves, and then lift to M. The problem with this argument is that there is no consistent way to define the vector fields on the union of the two red curves. But this is okay, as we can lift the definition on the individual red curves (as their preimages are disjoint critical manifolds in M), and define the vector field on M directly, ie the flow of the vector field on M cannot be made to be equivariant with respect to a flow on $\mathbb{R}^2$. □

We should point out that case 2 has one special case that does result in a homotopy type change. This is depicted in Figure 6(B). These types of 2–Morse functions are not
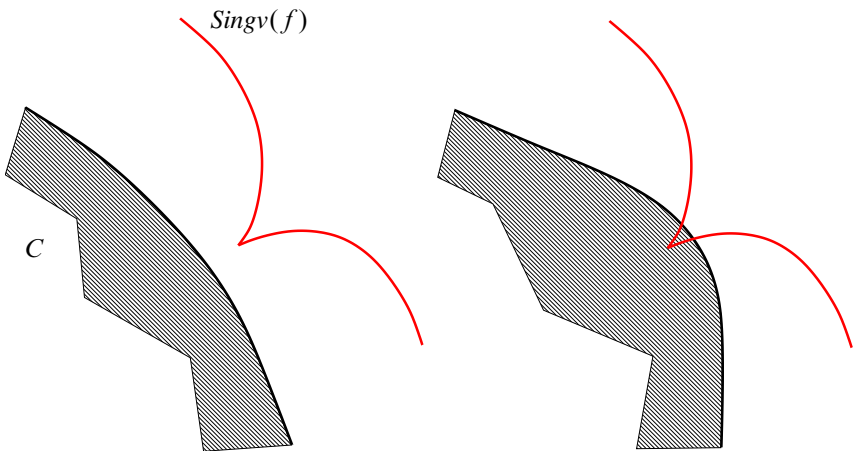
Figure 13: Case 2.
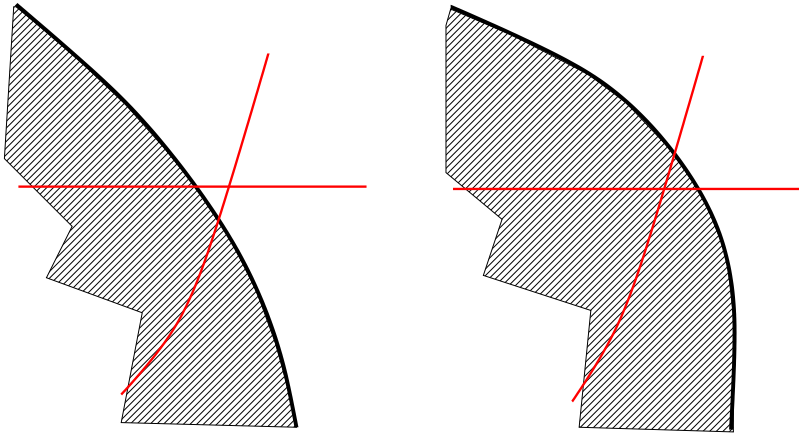
Figure 14: Case 3, over a double-point.

generic. A small isotopy of f allows one to ensure the tangent vectors at the cusps are neither vertical or horizontal, ie this at least codimension 1 in the space of smooth functions $M \to \mathbb{R}^2$, thus this situation is avoidable.

Theorem 2.9 allows us to draw the singular point set of the filtration M_f from the singular values of f, allowing automatic deduction of Examples 2.4, 2.5 and 2.7. Specifically, the singular points of the filtration are the Pareto curves of the defining map f together with the relevant vertical and horizontal rays (extending to $+\infty$) at the corresponding vertical and horizontal tangent points.

An analogous result to Theorem 2.9 appears in [2].

Proposition 2.10 *We summarize the cell attachments at the singular values of the filtration M_f.*

- *For corner singular points, the index of the cell attachment for M_f is the same as the index for f.*

- *[28] For tail singular points, if the singular values of f near the kissing tangency are exterior to the cube, then the cell attachment has the same index as f. This corresponds to Wan terminating a Pareto arc with a positive sign.*

- *[28] For a tail singular point, if the singular values of f near the kissing tangency are in the interior of the cube then the index of the cell attachment is one greater than that of the corresponding singular value for f. This corresponds to Wan terminating a Pareto arc with a negative sign.*

As a consequence of Theorem 2.9, the bifiltration of M associated to a 2–Morse function divides the plane into finitely many regions according to the homotopy type of the preimage $f^{-1}(C_{(a,b)})$. The notion of tameness [21] requires a further *no monodromy* condition, which is the requirement that there is a canonical isomorphism between $f^{-1}(C_{(a,b)})$ and a fixed representative for the region, and this isomorphism has to be natural in the sense that there is a canonical homomorphism between regions (if one exists). Our division of the plane is into contractible subspaces. By a cubical subdivision of the regions (akin to the argument that open subsets of the plane are triangulable), and taking a maximal tree in the dual 1–skeleton, one can construct a canonical zigzag of maps between any two points in a common region. The argument that there is no monodromy amounts to observing that the only avoidable handle attachments in a path from one region to another are cancelling pairs.

Corollary 2.11 [21] *Assuming the same conditions of Theorem 2.9, the bifiltration of $f\colon M \to \mathbb{R}^2$ is tame.*

We should note Wan [28] gives a filtration of the manifold M when $f\colon M \to \mathbb{R}^2$ is 2–Morse, provided the 2–Morse function satisfies the *no cycle* condition; see [28, Proposition 6.3]. Central to Wan's construction is the usage of flowlines of "generalized gradient" vector fields — roughly these are vector fields where both coordinates are increasing (away from the Pareto points). When one has a cycle, one can loop endlessly between Pareto points, but when there are no cycles, the process of connecting Pareto points via paths of generalized gradients exhausts the manifold M and linearly orders the critical intervals of Pareto sets. In our work there are a multitude of filtrations whether or not f has cycles. All the examples provided so far in this paper — and all examples in Wan's work [28] — satisfy the no cycle condition.

The simplest example of a 2–Morse function with a cycle in Wan's sense is a function of the form $f\colon S^1 \times D^2 \to \mathbb{R}^2$ having two critical arcs of index $(1,1)$, with the critical arcs being properly embedded in $S^1 \times D^2$. There are generalized gradient flows on the endpoints connecting the arcs in a cyclic ordering. While this function is only defined on a manifold diffeomorphic to $S^1 \times D^2$, with a little work one can embed this 2–Morse function into a closed 3–manifold, but one needs to add additional critical values. There is a rather simple cyclic example if one allows the use of 2–Morse functions of the sort $f\colon S^3 \to S^2$. We obtain this map as the composite of the 2–sheeted branched cover $S^3 \to S^3$ over the Hopf link together with the Hopf fibration $S^3 \to S^2$, provided the Hopf fibration projection of the Hopf link is a 2–crossing diagram in S^2.

3   Persistence paths and pathwise barcodes

In a 1–dimensional persistent homology, barcodes represent collections of parameter intervals at which homology generators are born and killed. In multifiltered persistent homology, in particular, in our 2–dimensional case, there is no simple barcode analogy, and, as Carlsson and Zomorodian pointed out in [8], there is no complete discrete invariant. Many authors have studied *rank invariants* in a module theory setting [8; 19]. A somewhat more elementary notion of *persistent Betti number* (*PBN*) *functions* is presented in Cerri, Di Fabio, Ferri, Frosini and Landi [10, Definition 2.2]. These are collections of functions $\{\beta_{f,q} : \Delta^+ \to N \cup \infty\}_{q \in \mathbb{Z}}$,

$$\beta_{f,q}((a,b),(a',b')) = \operatorname{rank} H_q(i^{((a,b),(a',b'))}),$$

where

$$\Delta^+ = \{((a,b),(a',b')) \in \mathbb{R}^2 \times \mathbb{R}^2 \mid (a,b) \preceq (a',b')\},$$

and $i^{((a,b),(a',b'))} \colon M_{(a,b)} \hookrightarrow M_{(a',b')}$ is the inclusion of sublevel sets.

For computational purposes, the authors of [10] use a reduction to one-dimensional persistence diagrams via so called *foliation method*. It consists of applying the one-dimensional rank invariant along the lines defined by positive coordinate vectors in chosen finite grids. That method is restated as a *fibred barcode* in the context of persistence modules by Lesnick and Wright [20, Section 1.5].

As we observed in Section 2 on our 2–Morse function examples, although there are uncountably many singular points, the changes in topology can be finitely characterised. They either occur when we cross an arc of the singularity *Singv* in the poset-increasing direction, or when we cross a horizontal or vertical half-line passing through the vertex (a,b) of $C_{(a,b)}$ and "kissing" the singularity. We will refer to both types of components of *Critv* as to *Pareto critical value arcs* or, for short, *Pareto arcs*. Note that in [28], the term *Pareto set* refers to a subset of *Singp* $\subset M$ and *critical intervals* to its components, while our Pareto arcs are the corresponding subsets of the extended Pareto grid *Critv* $\subset \mathbb{R}^2$. There are finitely many homotopically distinct paths, with $M_{(a,b)}$ starting with an empty set and ending with the whole manifold. Each one can give a different sequence of handle attachments creating new generators of homology or cancelling previous ones, all giving $H_*(M)$ at the end of the day.

This observation leads to the notion of persistence paths which is a substitute for either Cerri's foliation method [10] or Lesnick and Wright fibred barcode [20]. It can be also be viewed as a discrete analogy of Wan's generalized gradient (whose choice is also
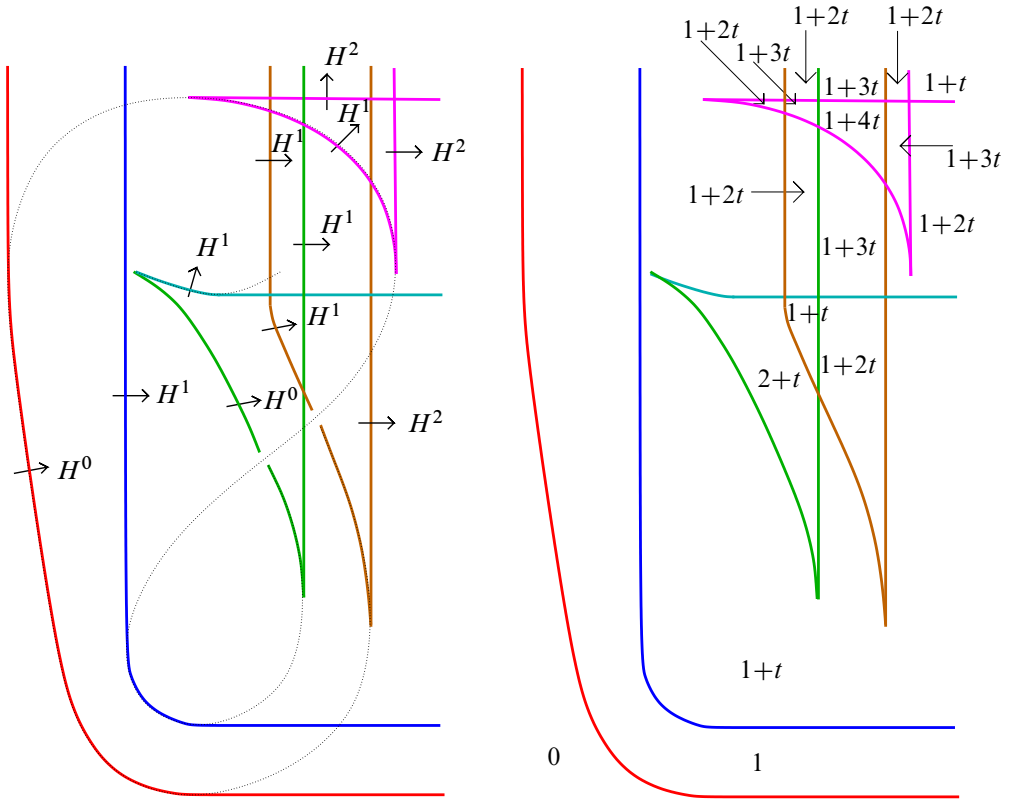
Figure 15: Klein bottle projection, with Poincaré polynomials.

not unique) in [28]. Before we proceed, let us introduce some terminology. As far as rank invariants or persistent Betti numbers are of concern, a convenient way to record the homological information carried in sublevel sets is the *Poincaré polynomial*

$$P(t, M) = \sum_{k=0}^{n} \beta_k t^k,$$

where $\beta_k = \text{rank } H_k(M)$ and n is the dimension of M.

In Figure 3 and Figure 15, left, we see the Poincaré polynomials $P(t, M_{(a,b)})$ for points (a, b) located in regions bounded by Pareto arcs. We are also interested in increments $\Delta P(t, H^j)$ arising as we cross a Pareto arc increasingly in (a, b). A j–handle can either create a j generator (new component, creating a hole or a cavity) or kill a $(j-1)$ generator (merging components, filling a hole or a cavity). In the first case, we get $\Delta P(t, H^j) = t^j$, and in the second case we get $\Delta P(t, H^j) = -t^{j-1}$. Thus the index

of a handle can be read out from ΔP. If it is t^k, we have a creating k–handle and if it is $-t^k$, we have a cancelling $(k+1)$–handle.

The term Pareto arc includes half-lines defined by quadrants $C_{(a,b)}$. Crossing their vertex (a,b) may create "multiple handles" where ΔP is not just one term. For example in the vertex of fish tail visible in Figure 16, $\Delta P = -t + t^2$. A point at which a single handle is attached will be called *generic*.

We choose a generic point (a,b) on each Pareto arc and let $H_{(a,b)}$ be the corresponding handle. At this time, the choice is arbitrary but we may want to chose endpoints of an arc, when we study metric sensitive barcodes.

We let $T = [0,1]$ and $R = [r_1, R_1] \times [r_2, R_2]$ be a fixed rectangle in $\mathbb{R}^2$ containing $f(M)$ in its interior.

Definition 3.1   Let $\{(a_i, b_i)\}_{i=0,1,\dots m} \subset R$ be a sequence of generic points on Pareto arcs such that $M_{(a,b)} = \varnothing$ for all (a,b) downward-left of (a_0, b_0), (a_{i+1}, b_{i+1}) can be reached from (a_i, b_i) going upward-right through the region enclosed by the two arcs, and $M_{(a_m,b_m)} = M$. A *persistence path* is a continuous function $\rho\colon I \to R$ with $\rho(0) = (r_1, r_2)$ and $\rho(1) = (R_1, R_2)$ which is nondecreasing in both coordinates, and joins the points of the sequence.

It can be seen that one can find sequences on the arcs so to get piecewise linear persistence (PL) paths with line segments between two consecutive points. This is useful in showing that we get a discrete characterization. For simplicity of notation, we let $H_i = H_{(a_i,b_i)}$ and $M_i = M_{(a_i,b_i)}$. We have a linear filtration

$$M_0 \subset M_1 \subset \cdots \subset M_m = M.$$

Figure 16, left, shows two persistence paths for the cupped sphere presented in Example 2.5. The path displayed in dark green avoids the pocket, the one in orange passes through it.

Note that [28] needs a no-cycle condition to apply the generalized gradient. Our persistence paths can be defined even in the presence of Wan's cycles, because they are more restrictive than Wan's admissible curves [28, Definition 6.3]: A persistence path leaves a Pareto arc at the same point as it enters it. Along the path, there may be no cycles, because it is increasing with respect to the poset relation.

We now shift our attention to a multidimensional analogy of the Morse inequalities. Our results may be useful for the continuation of the work on the discrete multidimensional Morse–Forman theory initiated in [1].
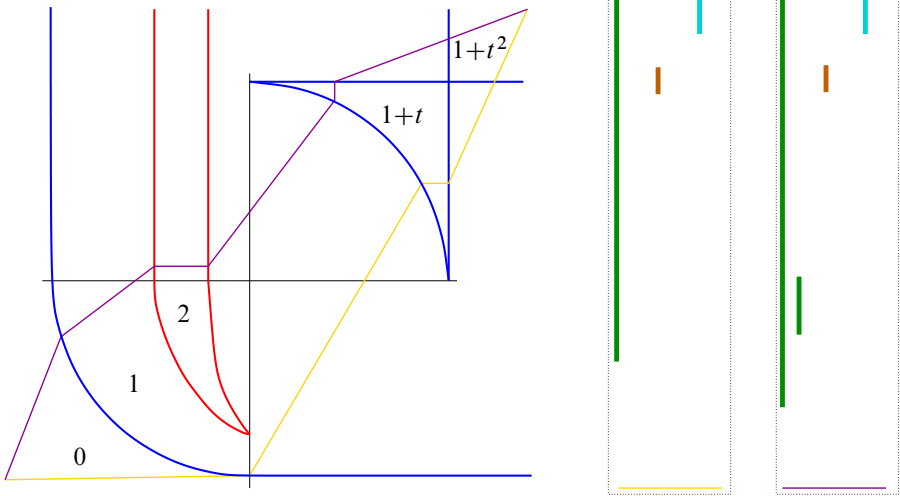
Figure 16: Left: two persistence paths for the function in Example 2.5. Right: their corresponding barcodes in rectangles marked with the same colour as the corresponding path; β_0 barcodes displayed by green lines, β_1 by brown lines, and β_2 by cyan lines.

The following result is an analogy of the Morse equation in the Conley index theory [23; 25].

Theorem 3.2 (Morse–Conley equation for persistence paths) *Let ρ be a persistence path for $((a_i, b_i))_{i=0,1,...m}$ and let c_j be the number of j–handles associated to its points. Then there exists a polynomial Q with nonnegative integer coefficients such that*

$$(1) \qquad \sum_{j=0}^{n} c_j t^j = P(t, M) + (1+t)Q(t).$$

Proof A direct consequence of the definition of ΔP and that of persistence path is

$$(2) \qquad \sum_{i=0}^{m} \Delta P(t, H_{(a_i,b_i)}) = \sum_{k=0}^{n} \beta_k t^k = P(t, M).$$

If all handles of ρ create new generators, then, in light of the preceding discussion, the left-hand side of (2) is exactly the left-hand side of (1). Thus (1) holds with $Q(t) = 0$. If a j–handle kills a $(j-1)$ generator, then the sum on the left-hand side of (2) misses two terms, t^{j-1} and t^j, contributing the sum on the left-hand side of (1). By adding all these missing terms to both sides of (2), we get (1) with Q built by terms $t^{j-1} + t^j = (1+t)t^{j-1}$. $\qquad\square$

By taking $t = -1$ in (1), we get the following corollary.

Corollary 3.3 (Euler characteristics) *For any persistence path ρ,*

(3)
$$\sum_{j=0}^{n}(-1)^j c_j = \chi(M),$$

where $\chi(M) = \sum_{k=0}^{n}(-1)^k \beta_k$ is the Euler–Poincaré characteristic of M.

Equation (3) is a part of the set of classical Morse inequalities. Since two polynomials are equal if and only if all their coefficients are equal, (1) also gives *weak Morse inequalities*,

(4)
$$c_j \geq \beta_j \quad \text{for all} \ \ j = 1, 2, \ldots n.$$

We conclude this section by deriving a classical result of Morse theory on *strong Morse inequalities*. The reader is referred to the book by Milnor [22] for the classical formulation. For the sake of completeness, we present a neat and short proof of an unknown source we have been told about by Marian Mrozek.

Corollary 3.4 (strong Morse inequalities) *For any persistence path ρ and any $k \geq 0$,*

(5)
$$c_k - c_{k-1} + c_{k-2} + \cdots \pm c_0 \geq \beta_k - \beta_{k-1} + \beta_{k-2} + \cdots \pm \beta_0.$$

Proof Knowing that $c_j = \beta_j = 0$ for all $j > n$, we can treat (1) as a power series equation

(6)
$$\sum_{j=0}^{\infty} c_j t^j = \sum_{j=0}^{\infty} \beta_j t^j + (1+t)Q(t).$$

Multiplying both sides of (6) by $\sum_{i=0}^{\infty}(-1)^i t^i$, the power series inverse of $(1+t)$, we get

$$\sum_{k=0}^{\infty}\left(\sum_{i=0}^{k}(-1)^i c_{k-i}\right)t^k = \sum_{k=0}^{\infty}\left(\sum_{i=0}^{k}(-1)^i \beta_{k-i}\right)t^k + Q(t).$$

Since two power series are equal if and only if all their coefficients are equal and the coefficients of $Q(t)$ are nonnegative, we get (5). $\square$

Our Morse inequalities should be compared with the work of Wan [28]. Perhaps the main difference between our work and his is that we convert functions $f\colon M \to \mathbb{R}^2$ into families of filtrations of the manifold M. Wan uses essentially all of the Pareto arcs to define his filtration, which is often larger than our filtrations. Moreover he

requires special "acyclic" Morse 2–functions to even define a filtration of M, while any Morse 2–function works for us.

We now turn our attention to the computability of persistent homology via persistence paths. We associate *pathwise barcodes* to any persistence path ρ as follows. First, we want to normalise lengths of persistence paths so to have them all of length 1. Given a point $(a, b) \in \rho(I)$, let $s(a, b)$ be the euclidean distance from (r_1, r_2) to (a, b) along the path ρ divided by the total length of ρ.

Definition 3.5 The ρ–*barcode* in homology of dimension k is a function on representatives of the H_k generators, whose values are subintervals of $[0, 1]$. When an H_k generator is born by a handle attachment at the point (a_i, b_i) and it is killed at the point (a_j, b_j) with $i < j < m$, the corresponding barcode interval is $[s(a_i, b_i), s(a_j, b_j)]$. The *lifetime* of that generator is $s(a_j, b_j) - s(a_i, b_i)$. If a generator persists until the point (R_1, R_2) of the chosen rectangle, it will also persist if the values of (R_1, R_2) increase. Thus it is reasonable to declare that its lifetime is infinite and the corresponding barcode interval is $[s(a_i, b_i), \infty)$.

Figure 16, right, shows barcodes of the two persistence paths displayed on the right. It is visible that the lifetime of the second generator of H_0 created when crossing the pocket is short and it may be null, if we choose the path in dark green that avoids the pocket. Similarly, the lifetime of the H_1 generator is short.

We shall now briefly discuss prospects for numerical implementations of pathwise barcodes. We should emphasize that the aim of our paper is to only provide a theoretical background for computation.

Following predecessors [8; 10] who set up computing methods for multifiltrations, we should consider the family of all piecewise linear persistence paths ρ built on points (a_i, b_i) in a given finite grid. However, that is a huge family and this choice is likely to lead to computational complexity issues. The size of the family of such paths is most likely similar to that of *Young diagrams* [13]. Moreover, the number of nodes to join by paths, decisive for the size of the family, increases quadratically with grid subdivisions.

For pathwise barcodes, we postulate that it should be sufficient to consider a finite representable family $\mathrm{Rep}(f)$ of persistence paths built of specific points on Pareto curves: centre points, nearly lower-right and upper-left endpoints of Pareto curves, as well as their intersections with horizontal and vertical lines passing through or touching other endpoints. We claim that $\mathrm{Rep}(f)$ is a small and exhaustive representation. Moreover, the size of $\mathrm{Rep}(f)$ does not increase with grid subdivisions.

By *exhaustive representation*, we mean here that any additional paths give rise to *equivalent barcodes*. That, in turn, means that their barcodes have the same number of intervals for each homology dimension, they may vary by length but appear in the same sequence according to birth and death dates.

We are conscious of the fact that, proceeding this way, we are missing the postulate that the persistence should be computed blindly from data, without knowing the exact manifold M and exact function f. But it may also be interesting to consider the case when we have M and f given by formulas that enable computing singularities.

4 Extensions

When applying pathwise barcodes to functions which do not satisfy Wan's no-cycle property [28, Definitions 6.4 and 6.5], it would be interesting to see what is the information carried by the barcodes of those persistence paths of $\operatorname{Rep}(f)$ which cross and go about the cycles of f.

The filtration of $\mathbb{R}^2$ by quadrants $C_{(a,b)}$ has a complementary filtration by quadrant exteriors
$$E_{(a,b)} = \{(x, y) \in \mathbb{R}^2 \mid x \geq a \text{ or } y \geq b\}.$$

Provided the boundary of $C_{(a,b)}$ is transverse to the singular points of $f \colon M \to \mathbb{R}^2$, one has that $f^{-1}(C_{(a,b)})$ is a manifold with corners. This allows us to use a Poincaré duality isomorphism
$$H_k(f^{-1}(C_{(a,b)})) \simeq H^{m-k}(M, f^{-1}(E_{(a,b)})).$$

Given that quadrant exteriors are the union of three quadrants, this gives a fairly detailed relationship between the persistent homologies of filtrations corresponding to the four quadrant families:
$$C_{f_1 \leq a, f_2 \leq b} = C_{(a,b)}, \quad C_{f_1 \geq a, f_2 \leq b}, \quad C_{f_1 \leq a, f_2 \geq b}, \quad C_{f_1 \geq a, f_2 \geq b}.$$

This technique could be thought to be a strong parallel to the theory of trisections of 4–manifolds [14; 15] as developed by Gay and Kirby. It also gives a formal setup analogous to *extended persistence* of Morse functions, considered in [12].

Another direction one could take to extrapolate this research would be using smooth functions $M \to \mathbb{R}^k$ for $k > 2$. This topic is of a great interest to the topological data analysis community. The computational methods of multiparameter persistent homology such as those in [1; 8; 9; 19] are dimension-independent but, on the other hand, they do not have the same insight into the geometry of the encountered singularities as the

one we present here for the $\mathbb{R}^2$–valued functions. There are a variety of useful "Morse theory" type tools to describe the singularities of functions of this kind. The analogous theory of multisections of manifolds is developed by Rubinstein and Tillman [24].

Yet another direction to undertake is the practical implementation of our suggested method for computing pathwise barcodes on the basis of a representable family Rep(f).

References

[1] **M Allili**, **T Kaczynski**, **C Landi**, **F Masoni**, *Acyclic partial matchings for multidimensional persistence: algorithm and combinatorial interpretation*, J. Math. Imaging Vision 61 (2019) 174–192 MR Zbl

[2] **M Assif P K**, **Y Baryshnikov**, *Biparametric persistence for smooth filtrations*, preprint (2021) arXiv

[3] **A Banyaga**, **D Hurtubise**, *Lectures on Morse homology*, Kluwer Texts in the Mathematical Sciences 29, Kluwer, Dordrecht (2004) MR Zbl

[4] **S Biasotti**, **A Cerri**, **P Frosini**, **D Giorgi**, **C Landi**, *Multidimensional size functions for shape comparison*, J. Math. Imaging Vision 32 (2008) 161–179 MR

[5] **R Bott**, *Lectures on Morse theory, old and new*, Bull. Amer. Math. Soc. 7 (1982) 331–358 MR Zbl

[6] **P Bubenik**, **M J Catanzaro**, *Multiparameter persistent homology via generalized Morse theory*, preprint (2021) arXiv

[7] **F Cagliari**, **B Di Fabio**, **M Ferri**, *One-dimensional reduction of multidimensional persistent homology*, Proc. Amer. Math. Soc. 138 (2010) 3003–3017 MR Zbl

[8] **G Carlsson**, **A Zomorodian**, *The theory of multidimensional persistence*, Discrete Comput. Geom. 42 (2009) 71–93 MR Zbl

[9] **N Cavazza**, **M Ethier**, **P Frosini**, **T Kaczynski**, **C Landi**, *Comparison of persistent homologies for vector functions: from continuous to discrete and back*, Comput. Math. Appl. 66 (2013) 560–573 MR Zbl

[10] **A Cerri**, **B Di Fabio**, **M Ferri**, **P Frosini**, **C Landi**, *Betti numbers in multidimensional persistent homology are stable functions*, Math. Methods Appl. Sci. 36 (2013) 1543–1557 MR Zbl

[11] **A Cerri**, **M Ethier**, **P Frosini**, *On the geometrical properties of the coherent matching distance in 2D persistent homology*, J. Appl. Comput. Topol. 3 (2019) 381–422 MR Zbl

[12] **H Edelsbrunner**, **J L Harer**, *Computational topology: An introduction*, Amer. Math. Soc., Providence, RI (2010) MR Zbl

[13] **W Fulton**, *Young tableaux: With applications to representation theory and geometry*, London Mathematical Society Student Texts 35, Cambridge Univ. Press (1997) MR Zbl

[14] **D T Gay**, **R Kirby**, *Indefinite Morse 2–functions: broken fibrations and generalizations*, Geom. Topol. 19 (2015) 2465–2534 MR Zbl

[15] **D Gay**, **R Kirby**, *Trisecting 4–manifolds*, Geom. Topol. 20 (2016) 3097–3132 MR Zbl

[16] **V Guillemin**, **A Pollack**, *Differential topology*, Prentice-Hall, Englewood Cliffs, NJ (1974) MR Zbl

[17] **A A Kosinski**, *Differential manifolds*, Pure and Applied Mathematics 138, Academic, Boston, MA (1993) MR Zbl

[18] **C Landi**, **S Scaramuccia**, *Relative-perfectness of discrete gradient vector fields and multi-parameter persistent homology*, J. Comb. Optim. 44 (2022) 2347–2374 MR Zbl

[19] **M Lesnick**, *Lecture notes for Math* 840: *Multiparameter persistence*, lecture notes, SUNY Albany (2019) Available at https://www.albany.edu/~ML644186/AMAT_840_Spring_2019/Math840_Notes.pdf

[20] **M Lesnick**, **M Wright**, *Interactive visualization of* 2–*D persistence modules*, preprint (2015) arXiv

[21] **E Miller**, *Homological algebra of modules over posets*, preprint (2020) arXiv

[22] **J Milnor**, *Morse theory*, Annals of Mathematics Studies 51, Princeton Univ. Press (1963) MR Zbl

[23] **M Mrozek**, *The Morse equation in Conley's index theory for homeomorphisms*, Topology Appl. 38 (1991) 45–60 MR Zbl

[24] **J H Rubinstein**, **S Tillmann**, *Multisections of piecewise linear manifolds*, Indiana Univ. Math. J. 69 (2020) 2209–2239 MR Zbl

[25] **K P Rybakowski**, **E Zehnder**, *A Morse equation in Conley's index theory for semiflows on metric spaces*, Ergodic Theory Dynam. Systems 5 (1985) 123–143 MR Zbl

[26] **O Saeki**, *Topology of singular fibers of differentiable maps*, Lecture Notes in Math. 1854, Springer (2004) MR Zbl

[27] **S Smale**, *Global analysis and economics: Pareto optimum and a generalization of Morse theory*, Synthese 31 (1975) 345–358 MR Zbl

[28] **Y H Wan**, *Morse theory for two functions*, Topology 14 (1975) 217–228 MR Zbl

[29] **H Whitney**, *On singularities of mappings of euclidean spaces, I: Mappings of the plane into the plane*, Ann. of Math. 62 (1955) 374–410 MR Zbl

Mathematics and Statistics, University of Victoria
Victoria, BC, Canada

Département de Mathématiques, Université de Sherbrooke
Sherbrooke, QC, Canada

rybu@uvic.ca, tomasz.kaczynski@usherbrooke.ca

See inside back cover or msp.org/agt for submission instructions.